

# Track Extrapolation and Distribution for the CDF-II Trigger System

Robert Downing, Nathan Eddy, Lee Holloway, Mike Kasten,  
Hyunsoo Kim, James Kraus, Christopher Marino, Kevin Pitts,  
John Strologas, Anyes Taffard

*University of Illinois at Urbana-Champaign,  
1110 West Green Street, Urbana, IL 61802, USA*

---

## Abstract

The CDF-II experiment is a multipurpose detector designed to study a wide range of processes observed in the high energy proton-antiproton collisions produced by the Fermilab Tevatron. With event rates greater than 1MHz, the CDF-II trigger system is crucial for selecting interesting events for subsequent analysis. This document provides an overview of the Track Extrapolation System (XTRP), a component of the CDF-II trigger system. The XTRP is a fully digital system that is utilized in the track-based selection of high momentum lepton and heavy flavor signatures. The design of the XTRP system includes five different custom boards utilizing discrete and FPGA technology residing in a single VME crate. We describe the design, construction, commissioning and operation of this system.

*Key words:* CDF-II Trigger, CDF-II Tracking

*PACS:* 07.05.Hd, 07.50.Qx

---

---

*Email address:* kpitts@uiuc.edu (Kevin Pitts).

## 1 Introduction

The CDF experiment was originally proposed more than 25 years ago. After several years of accelerator and detector construction, the CDF detector observed the first Tevatron  $p\bar{p}$  collisions in 1985. In the 20+ years since the first collisions were observed, the experiment has undergone several upgrades and completed several successful data runs, including Tevatron Run I from 1992-1996, which yielded the discovery of the top quark [1]. While the Fermilab Main Injector was being constructed in the late 1990's, CDF underwent a major upgrade, which included entirely new tracking systems, front-end electronics and a totally new trigger system. The first Tevatron Run II collisions were observed with the upgraded CDF-II detector in 2001. This paper documents the CDF Track Trigger Extrapolation System (XTRP), one of the components of the CDF-II trigger.

Central tracking has always been one of the strengths of the CDF experiment. The original CDF trigger included a three level architecture that included central tracking information at the second level. This tracking information was found to provide an extremely powerful handle for controlling trigger rates while maintaining high efficiency for physics signatures involving charged tracks. With Tevatron Run II upgrade anticipated to provide an instantaneous luminosity more than a factor of 10 higher than had been seen in Run I, it was clear that central tracking would need to play an even larger role in the CDF trigger strategy. This push for higher luminosity, coupled with continual developments in high speed digital electronics, led to a CDF II trigger design that featured high precision central tracking at the first trigger level, operating on every  $p\bar{p}$  collision.

In addition to finding charged tracks on every Tevatron bunch crossing, it is necessary to process those tracks so that trigger objects, such as electron, muon or heavy flavor candidates can be identified. This processing is performed by the XTRP system, which consists of fully custom digital boards residing in a single 9U VME crate.

This document describes the design, construction and operation of the XTRP system, which has been operating as a central component in the CDF II trigger system during Tevatron Run II. In the next section, we begin by providing an overview of the Tevatron, the CDF experiment and trigger system. In Section 3, we present the XTRP specifications and design concepts, as well as a detailed description of the components of the XTRP system. In Section 4, we describe the tools that were developed to test and commission this pipelined digital system. In Section 5, we describe the operation and performance of the XTRP system. We conclude in Section 6.

## 2 The Tevatron and CDF Experiment

The CDF-II detector is designed to study a wide variety of high energy processes produced by the Fermilab Tevatron proton-antiproton ( $p\bar{p}$ ) collider. With a bunch crossing rate of 1.7 MHz and a  $p\bar{p}$  collision rate as high as 10 MHz, it is necessary to perform significant event reduction. Less than 1 in 10,000 (0.01%) events can be stored for subsequent analysis, so a fast, efficient, intelligent trigger system is crucial to fully exploit the wealth of physics probed by these collisions.

This section provides information on the Fermilab Tevatron, as well as the CDF detector and trigger system. We attempt to present information relevant to help the reader understand the context in which the XTRP system was designed and operates.

### 2.1 The Fermilab Tevatron

The Fermilab Tevatron is a high-energy, high-rate ( $p\bar{p}$ ) collider that permits the study of the structure of matter at very small distance and very high mass scales. The CDF-II detector is a multi-purpose experiment specifically designed to study  $p\bar{p}$  collisions at the Tevatron. The CDF-II detector utilizes precision tracking and calorimetry to identify and measure leptons, jets and heavy flavor ( $c$  and  $b$  quarks).

The first Tevatron/CDF physics run took place in 1987. Since then, both the accelerator and the experiment have undergone multiple rounds of upgrades. After collecting  $110 \text{ pb}^{-1}$  of data in Run I, the Tevatron underwent a major upgrade which included the construction of the Main Injector and Antiproton Recycler [2]. During the same period, the CDF detector underwent a major upgrade to handle higher instantaneous luminosity and higher collision rates provided by the upgraded Tevatron [3].

Tevatron Run II began in March 2001 and will continue throughout much of this decade. In the Run II configuration, the Tevatron collides 36 proton bunches with 36 antiproton bunches with a bunch spacing of 396 ns. The bunch structure of the Tevatron has 3 bunch trains of 12 bunches each. Between the bunch trains are “abort gaps” of  $3.5 \mu\text{s}$  each, and the actual bunch crossing rate is 1.7MHz. The  $p$  and  $\bar{p}$  beam energies are 980 GeV, yielding a  $p\bar{p}$  center of mass collision energy of 1960 GeV. In July 2004, a peak luminosity of  $1 \times 10^{32} \text{ cm}^{-2}\text{s}^{-1}$  was achieved. At this luminosity, there are an average of 3  $p\bar{p}$  interactions per beam crossing. The ultimate instantaneous luminosity is expected to be  $3 \times 10^{32} \text{ cm}^{-2}\text{s}^{-1}$ , which corresponds to an average of 8  $p\bar{p}$  interactions per beam crossing.

## 2.2 The CDF-II Detector

The CDF-II detector has a cylindrical geometry, and therefore utilizes a cylindrical coordinate system, with the  $z$ -axis pointing in the direction of the proton beam,  $r$  the perpendicular distance from the beamline and  $\phi$  the azimuthal angle. It is also convenient to define  $\theta$  as the polar angle relative to the  $z$  axis, from which we use pseudorapidity, which is  $\eta = -\ln[\tan(\theta/2)]$ .

The Central Outer Tracker (COT) is a open-cell drift chamber that provides charged track identification in the central region ( $|\eta| \leq 1.1$ ) for tracks with transverse momentum  $p_T > 400 \text{ MeV}/c$  [4]. The COT has a cylindrical geometry of eight alternating axial and stereo superlayers. The active volume of the COT covers  $|z| < 155 \text{ cm}$  and 40 to 140 cm radius. The COT sits within a superconducting solenoid that provides a 1.4 T axial magnetic field.

Tracks found in the COT are extrapolated inward and matched to hits in the silicon microvertex detector for heavy flavor identification [6]. The microvertex detector provides precise three-dimensional track reconstruction, which is important for identification of long-lived particles.

Between the COT and solenoid is a time-of-flight system (TOF) for particle identification. Outside the solenoid are electromagnetic and hadronic calorimeters arranged in a projective-tower geometry, covering the pseudo-rapidity region  $|\eta| < 3.5$ . The central calorimeter consists of 24 “wedges” in azimuth, each wedge covering  $15^\circ$ . At a depth of  $\sim 6$  radiation lengths (shower maximum) within the electromagnetic calorimeters are wire chambers to precisely measure the shower position. An electron is identified as a track in the COT matched to a cluster in the electromagnetic calorimeter (with little or no hadronic energy) and shower maximum position consistent with the extrapolated track.

Outside the hadron calorimeters are drift chambers and scintillator counters for muon identification. The muon systems are segmented into four components, the Central Muon system (CMU) provides coverage for  $|\eta| < 0.6$  and  $p_T > 1.3 \text{ GeV}/c$ . The CMU follows the same 24-fold azimuthal symmetry as the central calorimeter. The Central Muon upgrade (CMP) covers the same pseudorapidity region as the CMU, but sits behind an additional  $\sim 3$  interaction lengths of material, providing identification for muons with  $p_T > 3 \text{ GeV}/c$ , with higher purity than muons identified only in the CMU. The Central Muon extension (CMX) provides coverage for  $0.6 < |\eta| < 1.1$  and  $p_T > 2.0 \text{ GeV}/c$ . The Intermediate Muon system (IMU) provides coverage for  $1.1 < |\eta| < 2.0$  and  $p_T > 3.0 \text{ GeV}/c$ . Muons are identified as tracks in the COT matched to track segments in one or more of the muon systems.

## 2.3 The CDF-II Trigger System

The CDF-II data acquisition system can store data at a maximum rate of 18 MB/s. With an average event size of 170 kB, this translates into an event rate of 100 Hz. Therefore, in processing the 1.7 MHz of collision data, the CDF-II trigger system must reject more than 99.99% of the events. In order to maintain high efficiency for interesting signatures, the trigger system must be fast, flexible and operate with low deadtime. Central tracking plays a crucial role in the CDF-II trigger, allowing for the identification of high  $p_T$  electrons, muons, tau leptons, and daughter tracks from heavy flavor decays.

The CDF-II trigger system has a three-level architecture with each level providing a rate reduction sufficient to allow for processing at the next level with minimal deadtime. Level-1 operates on every beam crossing and uses custom designed hardware to find physics objects based on a subset of the detector information and makes a decision based on simple counting of these objects (*e.g.* one 12 GeV/ $c$  electron or two 1.5 GeV/ $c$  muons). The Level-2 trigger uses custom hardware to do a limited event reconstruction which can be performed in a single programmable processor. The Level-3 trigger uses data from full detector readout to fully reconstruct events in a farm consisting of more than 100 commercial dual processor PCs.

The functionality of the three level pipelined and buffered trigger system is shown in Figure 1. Although the time between collisions is 396 ns, the base CDF-II clock period utilized by the entire CDF trigger system (CDF\_CLOCK) is 132 ns. The original specification for the CDF-II detector allowed for operation with a Tevatron bunch spacing of 132 ns, and consequently the CDF-II trigger and data acquisition system was built to operate in both 132 and 396 ns configurations from a base system clock period of 132 ns. To allow time for transmission and processing of the trigger signals, there is a 5.5  $\mu$ sec Level-1 latency from  $p\bar{p}$  collision to Level-1 trigger decision. This requires each detector element to have local data buffering for 42 clock cycles.

If an event is accepted by the Level-1 trigger, all front-end readout components move the data to one of four on-board Level-2 buffers. This buffering is sufficient to average out the rate fluctuations and allow a 25 kHz Level-1 accept rate with  $\leq 5\%$  deadtime for the average of 35  $\mu$ sec Level-2 processing time. An event which satisfies the Level-2 trigger undergoes full detector readout, and the data from each of the front-end elements is assembled into a single event which is fed to one of the processors in the Level-3 computing farm. Detector readout, the event builder and Level-3 computing farm provide sufficient bandwidth to permit the Level-2 trigger to accept events at a rate of 350 Hz. In the Level-3 trigger processor farm, the events are reconstructed and filtered using full event reconstruction, with 75 Hz written to permanent

storage. The peak achieved rates are 15-25% higher than the typical operating trigger rates listed here.

The block diagram for the CDF II trigger system is presented in Fig. 2. The input to the Level-1 hardware comes from the calorimeters, tracking chamber, and muon detectors. The decision to retain an event for further processing is based on the number and energies of track, electron, photon, muon,  $\tau$  lepton and jet candidates, as well as the total energy and missing transverse energy in the event. The Trigger Supervisor System (TSI) is responsible for maintaining synchronization and allocating buffer space for each event accepted at Level-1 [3].

Since the Level-1 and Level-2 trigger systems each require rejection factors of  $\sim 70$ , they need significant detector information to perform their function. Several detector systems provide information for the Level-1 trigger decision: the calorimeter (CAL), COT, CMU/CMX/IMU systems (MUON), TOF, Cerenkov luminosity monitor and Roman Pot detectors.

Two components add additional information in the Level-2 trigger system, the Silicon Vertex Trigger (SVT) and the shower maximum wire chambers (CES). The SVT [5] incorporates information from the high precision silicon microvertex detector [6] into tracking trigger selection. The SVT provides, for the first time in a hadron-collider experiment, the ability to trigger on displaced tracks arising from the decay of long-lived particles. This has already produced a number of new results involving hadronic decays of  $c$  and  $b$ -quarks [7].

All of the information available in the Level-1 trigger system in addition to data from the SVT and CES are brought together in the Level-2 decision crate (GLOBAL L2). The Level-2 decision node is the first place where software algorithms are utilized to process the event. For the first part of Run II, a DEC Alpha processor mounted on a custom 9U VME board was the Level 2 decision node. As part of a Level-2 trigger upgrade, the Alpha was replaced by a commercial PC processor utilizing a PCI interface. The Level-2 decision node is pipelined so that one event may be processed while the next event is being loaded.

#### 2.4 The XFT System

Track-based triggers (including lepton and heavy flavor triggers), account for approximately 75% of the CDF-II trigger bandwidth. The XFT system utilizes hit information from the COT to perform charged track reconstruction in the  $r$ - $\phi$  plane at Level-1. For tracks with  $p_T > 1.5 \text{ GeV}/c$ , the XFT system has high efficiency ( $> 90\%$ ), good transverse momentum resolution,  $\delta p_T/p_T = 0.002 p_T$ ,

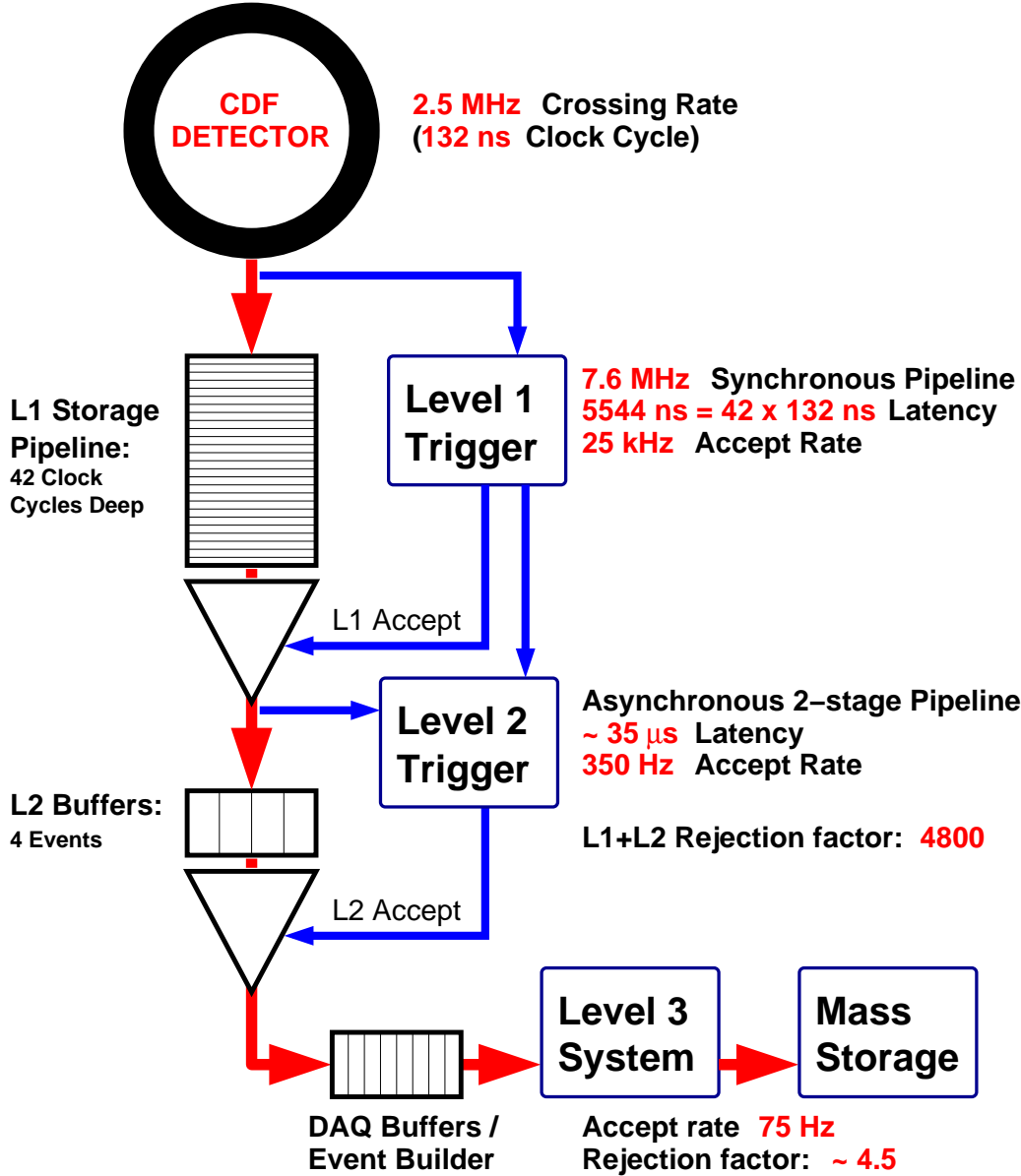
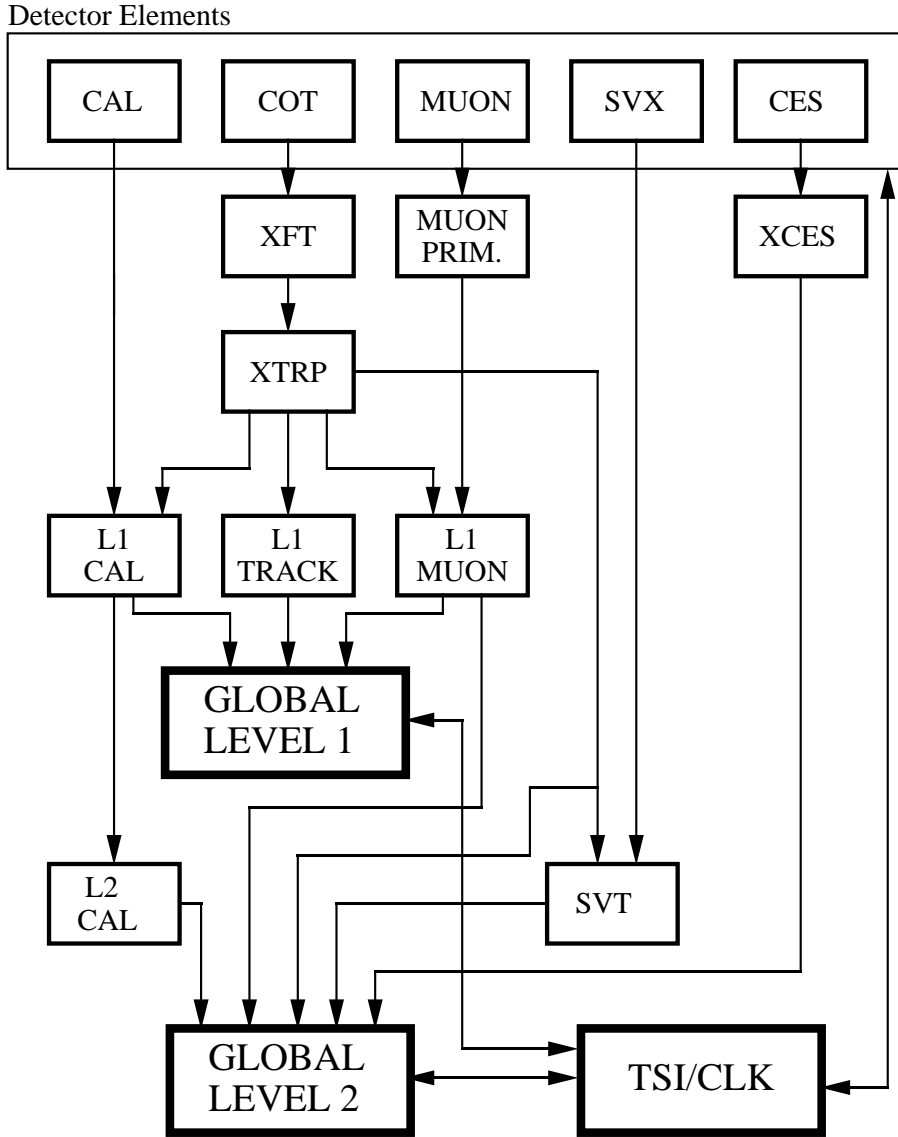


Fig. 1. The CDF-II trigger and data acquisition system. Data is acquired at the beam crossing period of 396 ns into a synchronous pipeline that is clocked at 132 ns. The Level-1 decision is produced after 42 clock cycles, at which point event processing becomes asynchronous. Typical trigger rates and rejection factors for the three-level system are shown in the figure.

and pointing resolution,  $\delta\phi_0 = 0.002$  radians, where  $\phi_0$  is the azimuthal angle of the track measured at the beamline ( $r = 0.$ ) [8].

The XFT logically divides the COT into 288 azimuthal segments, each covering  $1.25^\circ$ . These segments are processed in 24 XFT “Linker” boards, with each board covering  $15^\circ$  in azimuth. The segmentation is well-matched to the XFT angular resolution and the symmetry of the central calorimeter and CMU. The XFT reports no more than one track per segment. If more than one track

## **RUN II TRIGGER SYSTEM**



PJW 9/23/96

Fig. 2. The CDF-II trigger system. Trigger primitives are acquired from the detector elements and lead to a Level-1 decision. In the case of the track-based triggers, the XFT finds tracks in the COT, which are passed to the XTRP system. In the XTRP, the tracks are extrapolated to the muon and calorimeter systems for muon and electron identification. Tracks are also passed onto the Track Trigger (L1 Track) by way of the XTRP. The XTRP additionally provides tracking information for the Silicon Vertex Trigger (SVT) and Level-2 trigger processor.

is identified within a single  $1.25^\circ$  segment, the track with highest transverse momentum is reported.

Tracks found by the XFT are passed to the XTRP system, where the tracks are extrapolated to the calorimeter (L1 CAL) and muon systems (L1 MUON) for lepton identification. The XTRP also passes tracks to the Track Trigger (L1 TRACK), which selects events based upon trigger topology. If an event is accepted by the Level-1 trigger, the XTRP passes a complete list of tracks to the SVT and Global Level 2 systems.

### 3 The CDF Extrapolation (XTRP) System

In this section, we will describe the specifications for the XTRP system, the design and implementation of the system, the components and their interconnects. We begin with an overview of the system and its functionality, followed by a detailed description of each of the components of the system.

#### 3.1 XTRP Overview

The purpose of the XTRP is to receive tracking information from the XFT and distribute the tracks and information derived from the tracks to the Level-1 and Level-2 trigger subsystems. After receiving the tracks from the XFT, signals are sent to the Level-1 Muon system (L1 MUON), the Level-1 Calorimeter trigger (L1 CAL), and the Level-1 Track Trigger (L1 TRACK) as shown in Fig. 2. The tracks are also put into a storage pipeline and upon receiving a Level-1 accept are sent to the SVT and the Level-2 decision processor.

The XTRP system consists of a Clock/Control Board, twelve Data Boards, a Track Trigger Board, and two types of transition modules. The entire XTRP system resides in a single, 9U VME crate with a custom J3 backplane that satisfies the VIPA specifications [9]. The crate also contains a commercial VME CPU [10] and TRACER module which are common to all CDF-II VME crates. The TRACER (TRigger And Clock + Event Readout) is the gateway between the XTRP crate and the CDF-II trigger system. It receives CDF-specific timing signals as well as Level-1 and Level-2 Trigger Decisions [3].

For each Tevatron bunch crossing, the XFT reports information for all 288 azimuthal track segments to the XTRP. For the majority of the segments, the XFT reports that no track was found. Reporting a fixed amount of information on each bunch crossing lends itself nicely to the synchronous data processing performed in the Level-1 trigger system. Track finding in the XFT is complete  $2.7\ \mu\text{sec}$  after each  $p\bar{p}$  collision [8]. All of the XFT data is transferred to the XTRP in 132 ns.

The XTRP receives the track data from the XFT and, through the use of lookup tables, calculates the relevant information required by other systems to construct trigger objects. For example, muon primitives (track segments in the central muon chambers) are found at the same time the XFT is finding tracks in the COT. The XFT tracks are sent to the XTRP, which informs the Level-1 Muon trigger of all locations where a track extrapolates to the central muon systems. The definition of a muon object in the trigger is a track in the central muon system that is consistent with an extrapolated central track. Similarly, an electron is defined as a track plus an electromagnetic shower,

with the XTRP extrapolating the tracks into the calorimeter.

The following information is sent to the Level-1 trigger subsystems from the XTRP:

- **Central Muon systems (L1 MUON).** XFT tracks are extrapolated to the radii of the CMU, CMX and IMU. One or more bits, corresponding to  $2.5^\circ$  azimuthal segmentation, are set according to  $p_T$ ,  $\phi$ , and amount of multiple scattering. These bits are sent to the Level-1 Muon Trigger system. Two separate  $p_T$  thresholds are available for each of the three (CMU, CMX, IMU) subsystems.
- **Central Calorimetry (L1 CAL).** XFT tracks are extrapolated to Central Calorimeter towers. A set of four bits for each  $15^\circ$  wedge is sent to the Central Calorimetry Level-1 trigger. These bits correspond to four separate momentum thresholds.
- **Level-1 Track Trigger (L1 TRACK).** The Level-1 Track Trigger is an adjunct to the XTRP. It resides in the same VME crate and provides Level-1 triggers based on XFT track information only. The XTRP modules select tracks above a given  $p_T$  threshold and passes them on a bus to the Track Trigger. The total number of tracks is counted. If more than 6 tracks are found an automatic Level-1 accept is generated. If there are 6 tracks or fewer, the  $p_T$  and  $\phi$  information is used to interrogate look-up tables to generate up to 15 distinct Level-1 track-only triggers.

The XTRP must provide output information to the L1 CAL, L1 MUON and L1 TRACK systems within 300 ns of having received input XFT data. The L1 TRACK decisions must be available 396 ns after having received all of the input track data.

Upon receiving input data from the XFT, all segments are put into a pipeline and stored pending the Level-1 trigger decision. If a Level-1 accept is received the tracks are latched into Level-2 buffers. All non-trivial tracks are then extracted and put into two separate FIFO's for delivery to the Level-2 processor and to the SVT respectively.

An overview of the XTRP system can be seen in Fig. 3. In the following subsections, we provide a detailed description of the XTRP system.

### 3.2 Clock Control Board

The Clock Control Board has two primary functions: distribution of CDF-specific signals to the Data Boards and Track Trigger and interface with the Level-2 processor and the SVT.

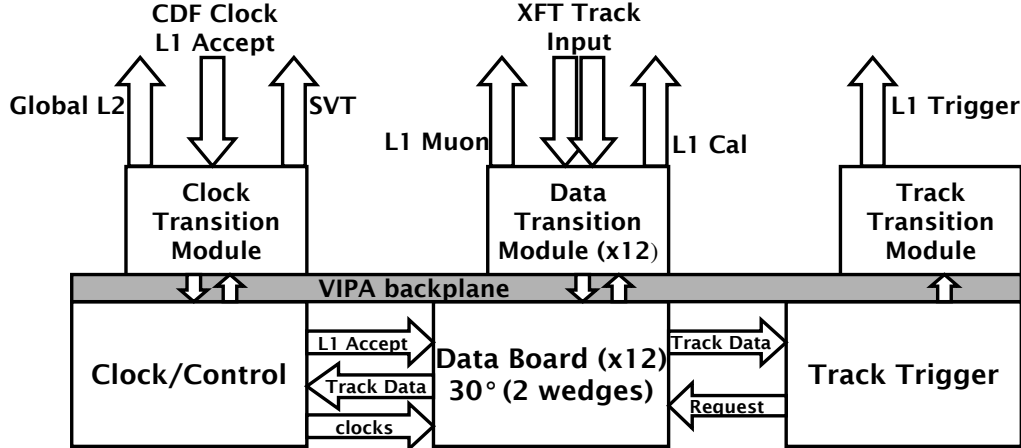


Fig. 3. An overview of the XTRP system. Each 9U VME board (Clock/Control, 12 Data Boards, Track Trigger) has an associated transition module. Horizontal arrows between the boards indicate data transferred within the system via the VIPA backplane. Vertical arrows within the backplane indicate pass-through I/O between the board and its transition module. Vertical arrows at the top of the picture indicate cables connections which are data interfaces with other trigger systems. All cables connect to the system through transition modules as shown in the figure.

The Clock/Control board receives the timing signals, including the 132 ns CDF\_Clock, and provides both 132 ns and 33 ns clock signals to the Data Boards and Track Trigger Board. The Clock/Control board can delay the output clock signals up to one full cycle in 3 ns increments. These variable delays are used to synchronize the XTRP system to the phase of the incoming track information from XFT. A fully programmable delay was implemented to account for uncertainty in the cable delays on the incoming track data.

Although a custom VME backplane was developed for CDF-II VME usage, the XTRP system utilizes a standard VIPA backplane. In a CDF-II VME backplane, signals are bussed across the P2 connectors, and may have clock skew of  $\sim 7$  ns from one end of the crate to the other. The VIPA backplane does not carry any common signals across the P2 connectors. In order for the Clock Control Module to receive the CDF-specific signals from the TRACER, a custom P2 transition card is installed opposite the TRACER. The signals are carried via connector to the Clock Control transition module and then fed through the backplane to the Clock Control module.

The 132 ns PECL CDF Clock signal is converted to TTL and passed through a programmable tap filter and Roboclock chip. This produces an even duty-cycle 132 ns clock signal. Additionally, a 16.5 ns clock signal is also generated to facilitate both the coarse delay of the 132 ns clock and generate an even duty-cycle 33 ns clock. The refined 132 ns and 33 ns clocks are multiplexed against signals, regulated by VME-access, that act as clocks. The effect is that

the XTRP system can run at real-time speed governed by CDF\_Clock or run as a large state machine, with each step interval under user control. The latter mode allows the user to “step” data incrementally through the system, while monitoring the data through each stage. This is described in Section 4.

The multiplexed clock signals are fanned-out on the Clock Control Board and fed to the custom backplane where each of the Data Boards and the Track Trigger receive a unique set of clock signals. With trace length matching, the skew for these signals less than 1 ns across all of the boards.

For every Level-1 accept the Clock Board must send a list of tracks to the Level-2 and SVT systems. This track list is created via a token ring initiated by the Clock Control board. The token ring is carried from board-to-board via the J5 connector on the custom J3 backplane. The Clock Board issues the token, which traverses the Data Boards and returns to the Clock Board. As the token arrives at each Data Board FPGA which holds the track data on the Data Board, the FPGA sends the track data across the custom backplane to the Clock Board. The Clock Board has two parallel on-board discrete FIFOs used to accumulate the track data. The FIFOs contain identical information, one sending the output to the Level-2 trigger and the other sending output to the SVT system. Data transmission is differential LVDS via ribbon cable. Since these transfers are variable length and asynchronous, it is terminated by an end-of-event word. Additionally, an 8-bit “bunch counter” is appended to uniquely identify the event. The value of this counter is compared with the expected value on the receiving end to verify that all parts of the system are processing the same event.

### 3.3 XTRP Track Input

On each event, track data for each wedge are sent from XFT to the XTRP system within a single 132 ns clock cycle. As mentioned previously, the XFT reports information for each segment regardless of whether a track is found or not. For each segment, 13 bits of track information are reported:

- **7 bits of transverse momentum ( $p_T$ ) information:** The XFT finds tracks with  $p_T > 1.5 \text{ GeV}/c$ . Track  $p_T$  values reported by the XFT are encoded into 96 bins, with bins 0-47 corresponding to negatively charged tracks and bins 48-95 corresponding to positively charged tracks. If no track is found in a given segment, its momentum bits are assigned a value of 124. The “short” tracks have a poorer  $p_T$  resolution, hence the  $p_T$  bin definitions are different for short tracks.
- **3 bits of “local  $\phi$ ”:** Each  $1.25^\circ$  segment is passed from the XFT to XTRP on a specific data bus, so the location of a segment in increments of  $1.25^\circ$  is

known by hardware location. In addition, three bits determine the azimuthal position of the track within the segment to an accuracy of  $\sim 0.16^\circ = 1.25^\circ/8$ . The reported azimuthal position of the track reflects the position of the track at a radius of 130 cm from the beamline.

- **1 isolation bit:** This bit was intended to indicate whether or not there were other tracks nearby in  $\phi$ . To date, this bit is unused.
- **1 “short track”:** This indicates that a found track did not pass through the outermost layer of the COT, denoting a track at larger pseudo-rapidity ( $|\eta| > 1$ ).
- **1 undefined bit:** This bit is reserved for future use.

These 13 bits of information are shipped from the XFT to the XTRP for all 288 segments for each event. The data are sent over 24 (one per wedge) 100-pin differential signal cables. The signal cables are bundled twisted pair, with a transmission length of 10 meters, terminated with subminiature D-style connectors. The data transmission is by differential LVDS format, synchronous with the 132 ns CDF clock. In addition to the segment information listed above, a “bunch 0” bit and 8-bits of bunch crossing number are sent on every cable to verify synchronization. To accomplish the transfer of an entire event every 132 ns, the data are 1-to-4 multiplexed and sent with a 33 ns clock. For a single event, 24 bytes are transferred per cable (corresponding to  $15^\circ$  in azimuth). Integrated over 24 cables, this translates into a data rate above 4 GB/s for the entire system.

The XFT data are received by the Data Board Transition Modules, which receive the differential LVDS signals and translate them to TTL before passing them through the P2 connector to the Data Board. There are eight Xilinx FPGAs on each Data Board which receive track information for each wedge. They are referred to as “Pipe” FPGAs because they decode and pipeline the incoming track data. Each Pipe FPGA handles track data for 3 XFT segments, so there are four Pipe FPGAs per wedge. The incoming track data for a single wedge are bussed to all four Pipes and each Pipe picks off the data it needs during each phase. Every 132 ns each Pipe assembles track data for three segments which are then ready to be processed.

### 3.4 Data Boards

The Data Boards perform the bulk of the functionality of the XTRP system. Each of the twelve boards handle  $30^\circ$  of the detector, corresponding to two  $15^\circ$  calorimeter wedges. On each clock cycle (132 ns) the Data Boards receive and decode incoming track data. The system receives a full event on each 132 ns clock-cycle. The data associated with non-collision clock-cycles is processed as a normal collision event, but trigger decisions are only relevant when there is

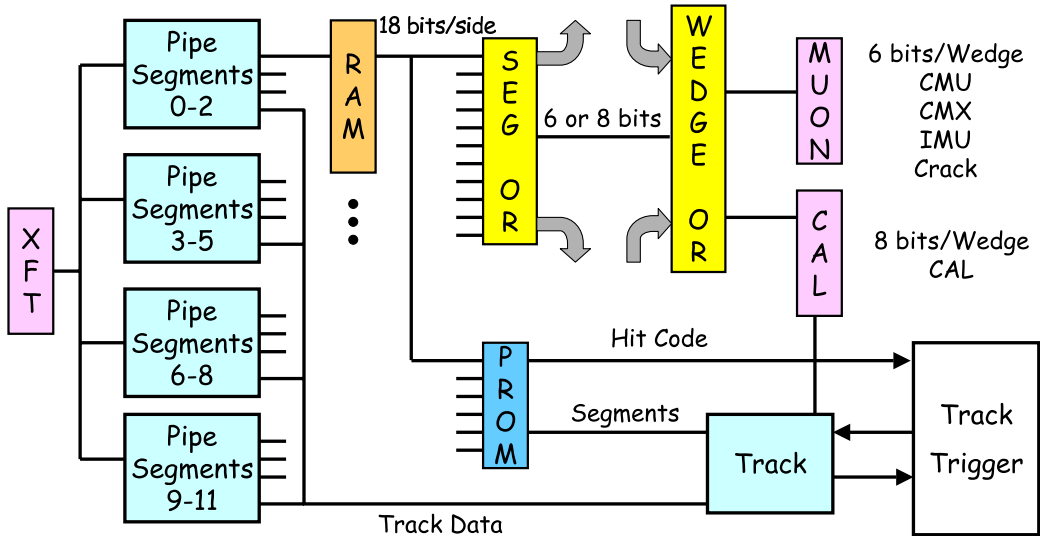


Fig. 4. Block diagram of the XTRP Data Board. Input data are demultiplexed in the Pipe FPGAs. The data are then presented to the lookup RAMs, followed by several stages of data compression as described in the text. The output stages and Track Trigger interface are responsible for shipping the data to other trigger systems.

a bunch crossing. Extrapolation information for muon and calorimeter trigger systems are also generated on each clock cycle. The Data Board processing time between the arrival of the track data and the production of extrapolation information is approximately 396 ns.

An overview of the Data Board functionality is shown in Figure 4.

Data Board function begins with the XFT track data being demultiplexed inside the Pipe FPGAs. The Level 1 pipeline for XFT track data are fully enclosed within the Pipe FPGAs. The pipeline depth is programmable up to 32 crossings ( $32 \times 132$  ns) after the data are received. The track data are stored until a Level 1 Accept/Reject decision arrives with information as to which, if any, Level 1 Decision Buffer the track data must be stored. The Clock/Control Board polls Level 1 Decision Buffer data from every Pipe FPGA into a FIFO, and sends the data to the Level-2 processor and the SVT.

### 3.4.1 Clocking

There are two distinct clock circuits on the Data Board: Oscillator Clock and CDF\_Clock. The Oscillator Clock circuit supplies a clock signal to all the FPGAs to perform VME-based transactions and run state machines within the FPGAs. The CDF\_Clock circuit provides the clocking for all the data

paths on the Data Board.

### 3.4.2 Extrapolating Tracks to Calorimeter and Muon Systems

The extrapolation of each track to the muon chambers and calorimeter is handled by lookup RAMs. Each Data Board has 24 lookup RAMS, one for each  $1.25^\circ$  segment within the  $30^\circ$  wedge covered by the Data Board. Each lookup RAM is  $32K \times 36$  with 15 address bits and the 36 output bits divided into two 18 bit outputs. Data pertaining to the Central Muon chambers (CMU) and Central Muon Extension chambers (CMX) are grouped into the “CM side” of the RAM. Data pertaining to the Intermediate Muon chambers (IMU), calorimetry (CAL), Track Trigger, TOF and  $\phi$ -gap bits are grouped into the “IM side” of the RAM.

The RAM contains the extrapolation data for every possible track. Once track data has been decoded for a segment, the 13 bits of track data along with 2 “phase” bits are presented as the address to a segment RAM. The phase bits are used to differentiate different lookup tables for different subsystems or different momentum thresholds. The data which are stored in the RAMs are generated and downloaded before each running period depending upon specified trigger parameters, and is discussed in Section 3.6. The 13 bits of track data remain fixed for a single event (132 ns) but the phase bits change every 33 ns. This provides four phases of output for every track. Given the dual output and four phases, eight separate lookups of extrapolation information are performed for each track, which are summarized in Table 1.

For the muon lookups: CMU, CMX, and IMU, each phase corresponds to a single  $p_T$  threshold. Each of the 18-bits of output information correspond to a  $2.5^\circ$  window in the muon system, so it is possible for a segment in one wedge to extrapolate to the adjacent wedges in the muon system. The  $\phi$ -gap and TOF lookups have two bits (low and high  $p_T$  thresholds) for each  $15^\circ$  wedge. The Calorimeter lookup provides 16-bits of information, which is 8  $p_T$  thresholds mapped to a  $30^\circ$  window in the CDF-II Calorimeter. Since the Calorimeter trigger has  $15^\circ$  granularity, this extrapolation allows for tracks to extrapolate from one wedge into the nearest neighbor wedge. The Track Trigger output is a single bit per wedge which is used to determine which tracks are eligible for transfer to the Track Trigger Board, as described below.

### 3.4.3 Compression of Extrapolation Output

The result of each lookup (one per segment) is 18-data bits, corresponding to different  $p_T$  thresholds or detector  $\phi$  segmentation. Since nearby tracks can extrapolate to the same location in the detector, the extrapolation information must be compressed (“OR”ed) so that the ultimate output maps exactly

Table 1

Quantities extracted from the lookup RAMs. The 13-bit track data word is presented to the RAM for 132 ns, while the two phase bits cycle (00, 01, 10, 11 binary) each 33 ns. Each phase represents a different lookup on each “side” of the RAM. The output of each side is 18 bits of data, as described in the text.

lookup phase	CM side	IM side
0	CMU high $p_T$	Calorimeter (8 $p_T$ ) + Track (1 $p_T$ )
1	CMU low $p_T$	$\phi$ gap (2 $p_T$ ) + Time-of-Flight (2 $p_T$ )
2	CMX high $p_T$	IMU high $p_T$
3	CMX low $p_T$	IMU low $p_T$

onto the detector geometry. This compression is carried out through in series of stages. Data progresses through the stages in 33 ns cycles. Intra-wedge compression, among adjacent segments, is performed first, followed by inter-wedge compression, among adjacent wedges. The inter-wedge compression must handle adjacent wedges across adjacent Data Boards. The compression patterns are slightly different between calorimetry data and muon data. To save space on the Data Boards, the calorimetry and muon compression functions are performed by the same TTL/GTL translators with open-collector outputs for wire-AND logic.

All stages within the compression region are accessible to VME, and one can read the state of each compression stage for data verification. Furthermore, the VME access allows one to override the data presented to a subsequent stage with simulated data.

#### 3.4.4 Extrapolation Output

After compression stages, the data are sent by the Data Board through the backplane to the Data Board Transition Module. Calorimetry data for each 15° wedge are converted into a differential LVDS logic level before being sent to the Level-1 Calorimetry Trigger system [3] over two flat twisted pair cables, one cable per wedge. Muon data are input to a Channel Link chip [11] and passed in a quasi-serial format to the Level-1 Muon Trigger System over a single shielded twisted pair cable, terminated in an HD-20 connector. Both the L1 CAL and L1 MUON outputs are synchronized to the 132 ns CDF\_Clock.

#### 3.4.5 Track Trigger Interface

In parallel with extrapolating tracks to muon and calorimeter systems, up to two tracks per wedge may be sent to the Track Trigger board. Of the tracks that pass a single programmable  $p_T$  threshold, the tracks with the largest and

smallest  $\phi$  within a wedge are sent by the Data Boards to the Track Trigger board. The limit of two-tracks per wedge was necessitated by bandwidth issues. The choice of the two “outer” tracks (largest and smallest  $\phi$  within a wedge) was an algorithmic choice that best preserves the physics targeted by this trigger. The Track Trigger path within the Data Board provides the mechanism to select and transmit the desired tracks to the Track Trigger Board.

In the first lookup phase on the “IM” side, each RAM generates a single bit to indicate whether a track above a specified  $p_T$  threshold (typically  $2\text{ GeV}/c$ ) exists in the segment track presented to the Lookup RAM. On each Data Board the Track FPGA collects these bits and determines whether each wedge has 0, 1 or 2 tracks eligible to be sent to the Track Trigger. (As described above, a wedge with more than two eligible tracks is deemed to have two eligible tracks.) The Track FPGA then initiates a hand-shake with the Track Trigger. The information on the number of tracks per wedge (all 24 wedges) is accumulated by the Track Trigger board. The Track Trigger has lookup-RAMs to generate 3-bit codes which are returned to the Data Boards. The Data Boards then assert track data onto the time-multiplexed track data bus according to the codes generated by the Track Trigger.

On each Data Board, PROMs are used to discriminate the farthest separated tracks within a wedge that have asserted threshold signals. One set of PROMs, Code PROMs, outputs track quantity information based on the number of asserted threshold signals. A second set of PROMs, Address PROMs, outputs segment identification patterns. The Track Trigger board queries the Data Board for segment data. The Data Board sends the information for the track, in addition to the segment location, to the Track Trigger board.

### *3.5 The Track Trigger*

The Track Trigger board is the one board in the XTRP system that directly renders trigger decisions. These decisions are based upon tracking information only. Events selected by the track-only path at Level-1 provide heavy flavor candidate events for SVT trigger at Level-2.

Details of the interface between the Data Boards and the Track Trigger are described above. On the Track Trigger board, the track data are routed to a set of six “Sort” FPGAs. One half of these FPGAs is dedicated to extracting  $p_T$  data ( $p_T + \text{isolation} + \text{short track bits}$ ), the other half extracts the  $\phi$  data. From the wedge and segment origin of each track, a 9-bit “global  $\phi$ ” is generated ( $1.25^\circ$  segmentation). The local- $\phi$  information from the XFT is dropped.

The Track Trigger board receives a maximum of 6 tracks and must evaluate every possible two-track pair for the six tracks. This yields “6-pick-2” or 15 possible combinations of track pairs. Each of the the Sort FPGAs output data (segment or  $\phi$  information) for 5 pairs of tracks.

The data are fed to a bank of lookup RAMs. There are 15 unique  $p_T$  RAMS and 15 unique  $\phi$  RAMs, with each RAM corresponding to a specific track-pair. Trigger selection criteria are programmed into the RAMs. The lookup RAMs on the Track Trigger are  $512K \times 8$ , with 19 address bits and 8 data bits. Each track provides 9 bits to the lookup RAM, with the 19<sup>th</sup> bit used as a “phase” bit to generate two sets of 8 trigger bits. For every track-pair, the  $p_T$  and  $\phi$  lookup outputs are ANDed together to generate a trigger decision for that pair. All pairs are then ORed together to generate the trigger decision for the event. The RAMs output 8 decision bits every 66ns. The two 8-bit words are concatenated into a single 16-bit trigger word. Since one trigger bit is reserved for the auto-accept trigger (> 6 tracks) the Track Trigger is capable of generating 15 different track triggers. These 15 different triggers can be any combination of single-track and two-track selection criteria.

The resultant trigger data is piped to a Level 2 Buffer and fed through the backplane to the Track Trigger Transition Module. The trigger signals are converted to differential LVDS and sent to the global Level-1 decision crate over shielded twisted pair cable. The trigger signals are synchronized to the 132 ns CDF clock.

### 3.6 Interface With Trigger System

Since the extrapolation parameters may change during different running periods, the infrastructure was developed so that the values loaded in the lookup RAMs (both on the XTRP Data Boards and the Track Trigger Board) could be generated dynamically based upon the number and types of triggers utilized. In this section, we describe how the extrapolation parameters are generated and loaded into the XTRP system.

The Data Board lookup RAMs contain the information which takes an input track and extrapolates it to the calorimetry or muon systems. The extrapolation must account for the geometry of the detector, track curvature from the axial magnetic field and multiple scattering. The extrapolation formula used is the same for all detectors. The extrapolation determines a “window” bounded by a minimum and maximum value of  $\phi_{detector}$  within which a particle may be found. The extrapolation window is given by:

$$\phi_{detector} = K/p_T \pm \sqrt{(3\sigma_K/p_T)^2 + \sigma_a^2} + \phi_{XFT},$$

where the  $\pm$  values yield the maximum and minimum values of  $\phi_{detector}$  for a track that has a signed transverse momentum  $p_T$ . The terms  $K$ ,  $\sigma_K$  and  $\sigma_a$  are constants that depend on the detector subsystem. The term  $K/p_T$  accounts for the deflection of the track caused by the 1.4T solenoidal magnetic field,  $\sigma_K$  accounts for multiple scattering of the particle as it passes through the material of the detector, and  $\sigma_a$  is present to account for any misalignment between the COT and the detector to which the track is being extrapolated. The values of these constants are different for each one of the five detectors to which the XTRP extrapolates tracks. The extrapolation window, which is the middle term in the formula, allows for a 3-sigma multiple scattering term combined in quadrature with a misalignment term. See Table 2 for typical values utilized in extrapolation.

Table 2

Typical values used in XTRP extrapolation. The values of  $K$ ,  $\sigma_K$ , and  $\sigma_a$  are constants that were determined from data. The  $p_T$  thresholds are set in the trigger table and may change depending upon physics needs. In the case of the calorimeter trigger, electrons with a  $2\text{GeV}/c$  threshold are identified separately from positrons with a  $2\text{GeV}/c$  threshold. In all other cases, the charge of the track is not used to select leptons.

detector	$K$ ( $^{\circ}/(\text{GeV}/c)$ )	$\sigma_K$ ( $^{\circ}/(\text{GeV}/c)$ )	$\sigma_a(^{\circ})$	$p_T$ thresholds ( $\text{GeV}/c$ )
CMU	14.8	2.7	1.5	1.5, 4.0
CMX	13.36	5.39	1.5	2.0, 8.0
IMU	0	6.11	5	5, 11.
CAL	8.72	1.22	1.5	2.0+, 2.0-, 4.0, 8.0

The values for the constants described above were initially set using Monte Carlo simulations of the data, and the  $\sigma_a$  term was conservatively set to  $5^{\circ}$  for all triggers to ensure no events were lost. After the initial running period of CDF-II, data was used to refine the extrapolation constants. For the CMU and CMX optimizations,  $J/\psi$  data was used that came in on the CMU-CMU and CMU-CMX triggers respectively. The IMU trigger constants were examined using events with high momentum muons. For the calorimeter, generic tracks were used. Because the calorimeter segmentation is coarse ( $15^{\circ}$ ), and a track traverses very little material between the COT and the calorimeter,  $\sigma_K$  is quite small.

In addition to providing a  $\phi_{detector}$  window for extrapolated tracks, the XTRP also implements  $p_T$ , charge and short track selection criteria. The values of these cuts can change run-by-run and are set by the CDF-II trigger table. Typical momentum cut values are also summarized in Table 2.

To allow flexibility in the trigger definitions, the lookup tables utilized in the Data Boards are generated dynamically at the beginning of each run. This is

achieved by providing the relevant parameters to the initialization code, which in turn generates the lookup tables within the VME processor in the XTRP crate. This provides the additional advantage of transferring a small amount of data to the crate as opposed to downloading the large lookup tables over the network. On initialization, the XTRP VME processor is provided with the  $p_T$ , charge and short-track criteria from the trigger table and the extrapolation constants from a hardware database. From this information, the code generates 12 sets of extrapolation maps, one for each of the RAMs in an XTRP wedge. It then sends copies of the sets of maps to each of the 24 wedges, so that all of the 288 RAMs has the appropriate look-up table. It is only because the detector is nearly azimuthally symmetric and each XTRP wedge is identical that we need only 12 sets of maps; if necessary, we could generate 288 distinct lookups, one for each RAM. Since there is a 24-fold symmetry, to save time we have configured the system so that each lookup is simultaneously written to the 24 RAMs.

The Track Trigger lookups are generated in a manner analogous to that described above. For the Track Trigger, the trigger table provides the parameters and bit assignments for each of the triggers. The lookups are generated within the VME CPU and written to the lookup RAMs by VME block transfer.

## 4 XTRP System Testing

The XTRP system is designed with an eye toward testing and diagnosing system integrity. Functionally, the system is implemented via synchronous lookup rams and parallel pipelines stepping at 33ns. The design allows for VME readback of data at each stage in the pipelines which make possible sophisticated diagnostic and test procedures. These include basic functionality tests, full bit-by-bit tests, and full speed system tests. Within the trigger system, the XTRP is expected to provide reliable trigger information at a rate of 7.5Mhz with negligible error rates. This section describes the system features and software used to verify the system integrity and reliability, long before actual tracking data was available from the CDF-II detector.

All testing and diagnostic software was developed using CDFVME software framework. This package was developed to provide board and test stand software for CDF VME data acquisition and trigger system. It allows users to write java GUIs which communicate via ROBIN protocol with VxWorks C routines running on the VME front-end processor [12,13,14]. This enabled convenient development of Java-based graphical user interfaces (GUIs) while maintaining good system I/O performance on the VME front-end.

### 4.1 Basic Functionality Testing

All diagnostic and system testing software is based upon VME transactions with the XTRP system boards. With this in mind, the testing of each board is predicated upon a working VME interface. The VME interface is handled by a dedicated FPGA on each board which is loaded from a PROM at power-up. Each FPGA design contains a bank of test read/write registers to verify basic VME interface functionality and debug potential board level problems in the VME bus between the backplane and the VME FPGA. A reliable VME interface is required to load auxiliary FPGAs on the system boards and is the primary tool to probe basic functionality.

As noted in Section 3, on-board RAMs play a large role in the operation of the XTRP system. Before more sophisticated tests can be run, each RAM is exercised extensively to verify reliable operation. This consists of writing varied patterns and reading them back successfully from each RAM over thousands of trials.

On the XTRP Data Boards, the output of each RAM is the input into a GTL whose output is ORed onto a common bus. This first set of GTLs perform the intra-wedge ORing and are referred to as stage 0. As there are 12 GTLs which are ORed together onto this bus, it can be difficult to diagnose the source of

the problem if a bit error occurs on the stage 0 output. As part of the on-board diagnostics, the input to each GTL is tied to the VME bus. There are buffers which not only allow readback of the input of the GTL from the RAM under normal operation but also provide a means to bypass the RAM output and provide input to the GTL directly. Using these features, dedicated tests were developed to individually enable and test each bit independently on both the input and output sides of the GTLs, allowing for quick identification of any unreliable connections. Similar tests were developed and utilized to check the input and outputs of the inter-wedge ORing stages 1 and 2.

At the heart of the XTRP system is the system clock generated by the XTRP clock board. The clock functions in three basic modes - VME, normal, and burst. VME mode is used to generate the edges of the clocks (33 ns & 132 ns) via VME writes to a specified register on the clock board. This is only used for testing and diagnostics. In normal mode the clocks are free running and driven from the input system clock (CDF Clock). Finally there is burst mode in which a programmed number of clocks are generated after a given trigger event. Each of these modes play an important role in testing and diagnosing the XTRP system operation, and are discussed in detail below.

#### *4.2 Emulation*

To test the boards a full bit-by-bit emulation of each of the XTRP boards was developed. The emulation was written in java and provided classes for each board in the system to simulate all XTRP system functions including Level-1 trigger pipelines, Track Trigger, and Level-2 tracklists simultaneously. At the macro level, the emulation software is given track data input to each of its Data Board objects along with corresponding clock inputs and then provides all corresponding outputs as the data is clocked through the system. On a micro level, the emulation also provides full data for each pipeline throughout the system, from input to each RAM through each subsequent step of system. The emulation combined with the extensive VME diagnostic readback in the system provides a means to identify and diagnose board level problems in the entire system.

#### *4.3 VME Clock Tests*

The most thorough system tests are performed by using the VME interface to provide clock inputs to the XTRP system. In this scenario it is necessary to provide a method to input data into the system which is also easily controlled from VME to synchronize with the clocks. This is accomplished by taking advantage of the Pipe FPGAs on the Data Boards. Under normal operation,

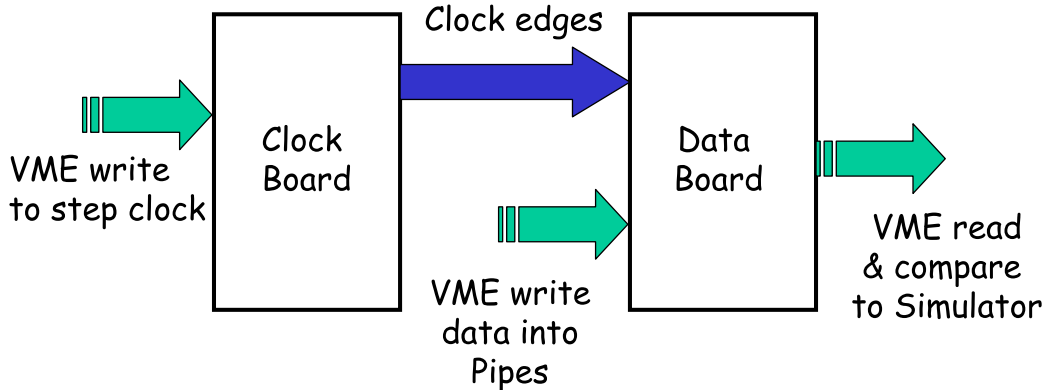


Fig. 5. Block diagram of the VME test procedure where data is manually inserted and stepped through the system under VME control.

these FPGAs receive incoming data from the transition modules, but in the VME test mode, they are switched to use input from internal VME writable registers. In this manner, it is possible to inject data and step it through the system entirely under user control via VME. A block diagram of the VME test is shown in Figure 5.

A complete GUI interface referred to as the “ExpertPanel” was developed to exercise the system under VME control. It interfaces not only with the XTRP hardware but also with the emulation software so that it can compare actual data in the boards to emulation expectations throughout the system. Figure 6, shows the main control display for the ExpertPanel. It provides control over system setup, input data, and clocks as well as an overview of the data to emulation comparison at each stage in the XTRP system. Each stage also has its own subpanel accessible via the tabbed panes at the top, which provides full bit-by-bit comparisons of the data at that stage in the board that can be used to pinpoint the exact location of any discrepancies. The drawback to this method is that it is very slow and it would take an incredibly long time to step large amounts of data through the system.

#### 4.4 Full Speed Testing

In order to increase the data bandwidth and test for timing related issues, the ability to process data with the Clock/Control Board and all system clocks operating at full speed was developed. At this speed data on the board is changing every 33 ns, so it is impossible to attempt to see what is happening by VME diagnostics. For full speed testing, data is input from an external source and the board outputs are subsequently logged and examined as shown in Figure 7.

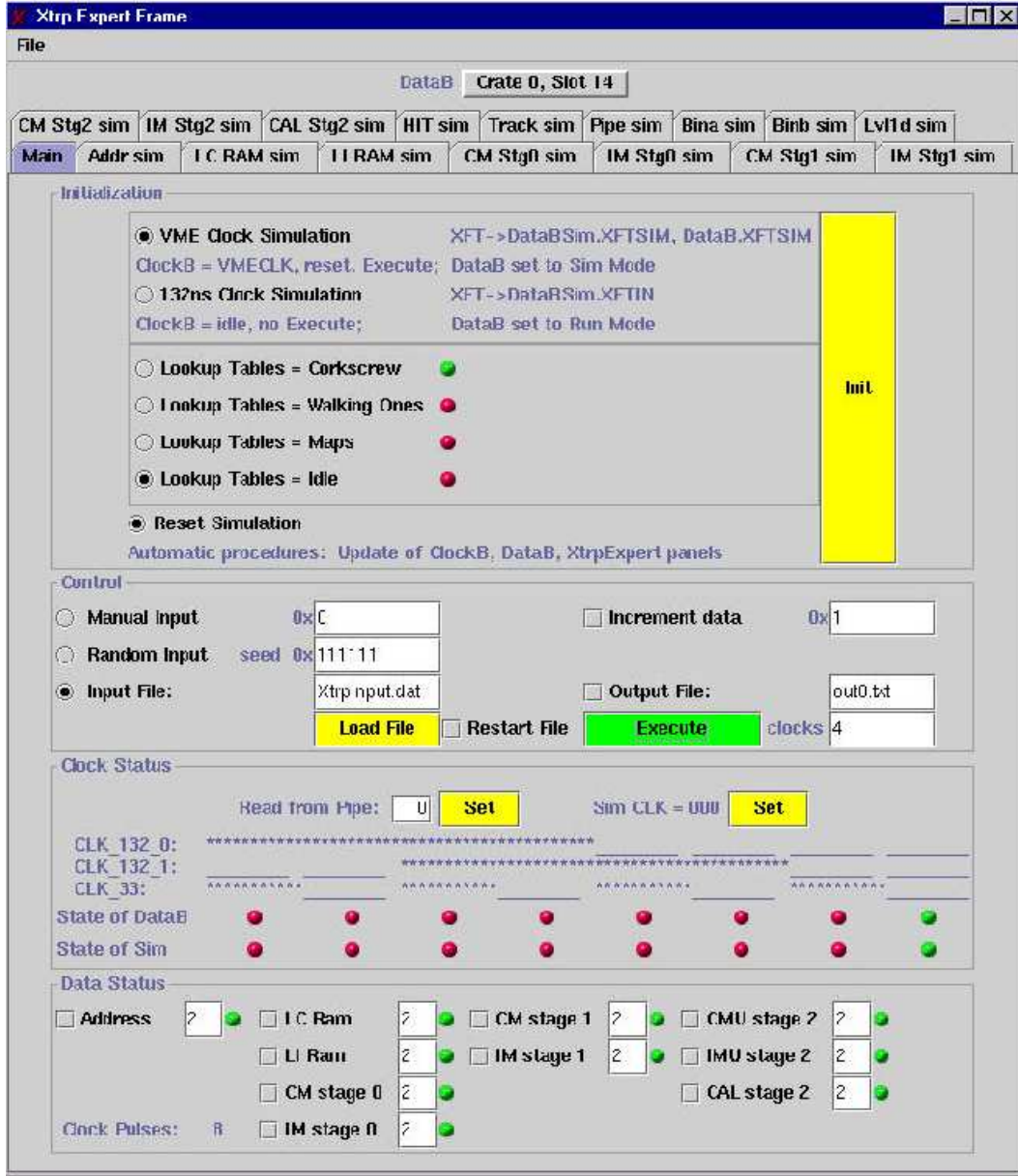


Fig. 6. Main display for the ExpertPanel diagnostic application. Allows the user to control configuration and setup while reporting on the status of hardware to emulation comparisons.

This required some additional test specific hardware which was developed for testing the XFT system. The LinkerTester, consists of a number of very large FIFOs tied to input and output channels and synchronized by the CDF Clock and programmable marker signals. Using this board, the output FIFOs can be configured to hold over 10k events for a single XTRP Data Board and are capable of capturing all the subsequent Level-1 trigger output.

Using the LinkerTester board, it was possible to run large amounts of data into the system at full speed and record the resulting trigger output which

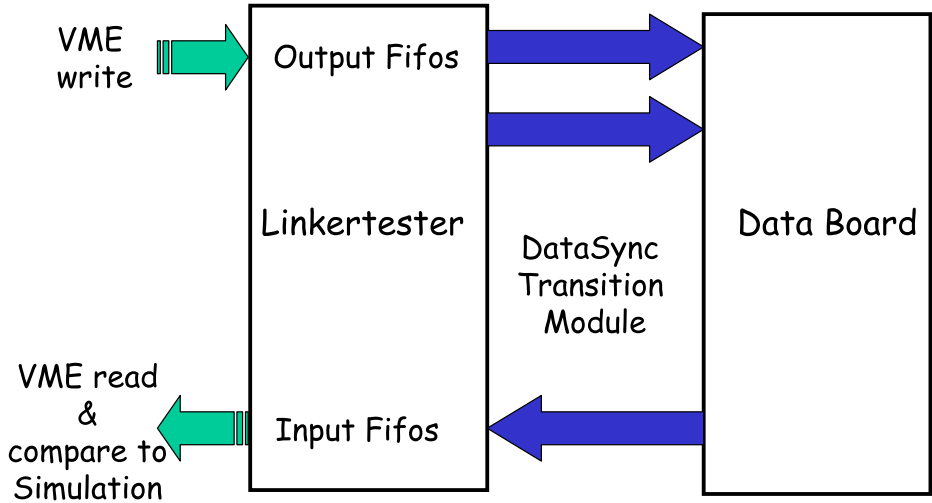


Fig. 7. Block diagram of test to insert and readback data from the system at full speed.

could be readback and checked against the expected emulation results. An application, referred to as LoopTest, was developed to continuously exercise the system at full speed and report any errors. This also exercises the full input and output path on the XTRP Data Boards which was not done by the VME tests.

LoopTest can run the system at full speed and determine if an error occurs in the output, but it does not provide any diagnostics about the error other than the input data which resulted in the error. It is then possible to input the same data at VME speed with the ExpertPanel to see if there is an error in the logic. If no error is observed at VME speed, then the error can be checked using the burst mode feature of the XTRP clock board. In this mode the system can be run at full speed for a programmable number of clock cycles and then halted so that the ExpertPanel can be used to readback the state of the board and compare to emulation expectations.

#### 4.5 Interface Testing

The final phase was to verify that the XTRP system was able to interface with other CDF-II trigger systems. As shown in Figure 2, the XTRP system receives its input from the XFT continuously and provides continuous output to Level-1 muon trigger, calorimeter trigger, and Level-1 global trigger. It also provides output to L2 trigger and SVT system when a L1 trigger accept is

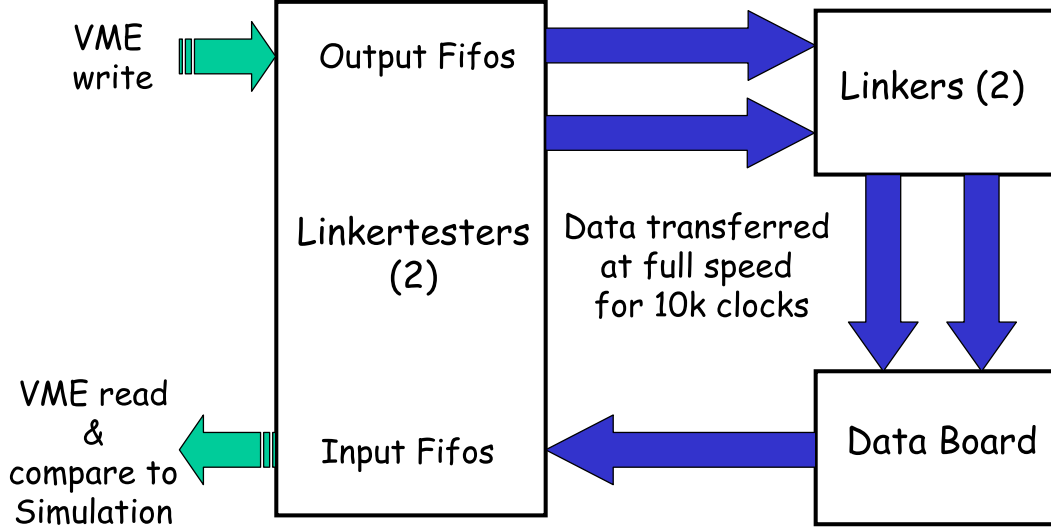


Fig. 8. Block diagram of the setup used to test the data interface between the XFT Linker and XTRP Data Boards.

issued.

The most extensive interface testing was done between the XFT Linker and the XTRP Data Boards. This link transfers a total of 1152 bits every 33ns over a total of 24 cables from 24 different Linkers into 12 XTRP Data Boards where they all must be latched at the same time to keep the data synchronized. This required extensive testing to determine the optimal timing settings for the system and insure reliable data transfer. The LinkerTester, being originally designed to test the XFT Linker boards, was used to perform these tests. The optimal timing settings were determined by attaching a logic analyzer to the incoming signals and adjusting the XTRP system clock using the delays on the cdf clock board. Reliability tests were then performed by running large volumes of data through both the Linker and XTRP using the LinkerTester as shown in Figure 8.

The output interfaces were much simpler and were exercised during the initial testing but did not get fully exercised until all the trigger systems were installed in the CDF-II system. This was done during commissioning of the CDF-II detector and electronics. The XTRP system became a valuable tool during this period. A new design for the pipe FPGAs on the Data Boards was developed which allowed for simulated track data to be input and run through the system. With beam time for testing at a premium, this proved an invaluable tool not only for interface tests but for testing and commissioning track based triggers throughout the system.

#### *4.6 System Timing*

As described above, the relative timing between the XFT and XTRP systems was well measured in the test stand. At the time of installation of the trigger system, the overall system timing was known relatively well (to within  $\pm 1$  clock cycle) based upon a detailed accounting of measured latencies and cable delays. The overall system timing was then verified using colliding beam data, where events were read out on four consecutive clock cycles. By comparing the data for each subsystem in each of the four events, the final timing of the system could be established and set. This technique was straightforward because of the detailed accounting performed prior to operation. Once the system was fully timed-in, the timing has been stable and robust.

## 5 Operations

The XTRP system was installed and commissioned during the Summer 2001. It was fully functional for the CDF-II physics run that began in January 2002.

### 5.1 Maintenance and Reliability

The reliability of the system has been quite high. In 3.5 years of running, there have been two single-component failures on Data Boards, and zero failures on any of the other boards in the system. In both cases of Data Board component failure, the board was replaced while it was repaired.

System maintenance has been successful for three reasons:

- (1) This digital system can be fully emulated to quickly identify problems.
- (2) The testing software described in the Section 4 make it possible to quickly isolate the source/location of an error.
- (3) The XTRP system is located away from the beamline, so it can be accessed at any time without loss of colliding beams.

In the following section, we describe the emulation and monitoring tools that are utilized in this system.

### 5.2 Monitoring: XTRPSim and XTRPMon

As described in Section 4, we are able to fully emulate the performance of this digital system. We have constructed a software package, known as XTRPSim, which can use data from the detector (or data from simulated events) to fully emulate the XTRP system. This digital emulation was utilized heavily during system development and commissioning, and was then ported to the CDF-II analysis environment so that it could be utilized while the experiment is running.

During data-taking, a random sampling of events are fed to the “monitoring stream” at a rate of 1Hz. These events are fully emulated using the XTRP-Sim. The results of the emulation, along with the data, are then passed to XTRPMon, which performs several checks on the data. XTRPMon performs bit-for-bit comparisons between XTRP data and the XTRPSim emulation. In addition, many relevant pieces of trigger information are read out at different locations in the trigger chain. These can be compared to one another to check for data link integrity. For example, the XFT track data is available

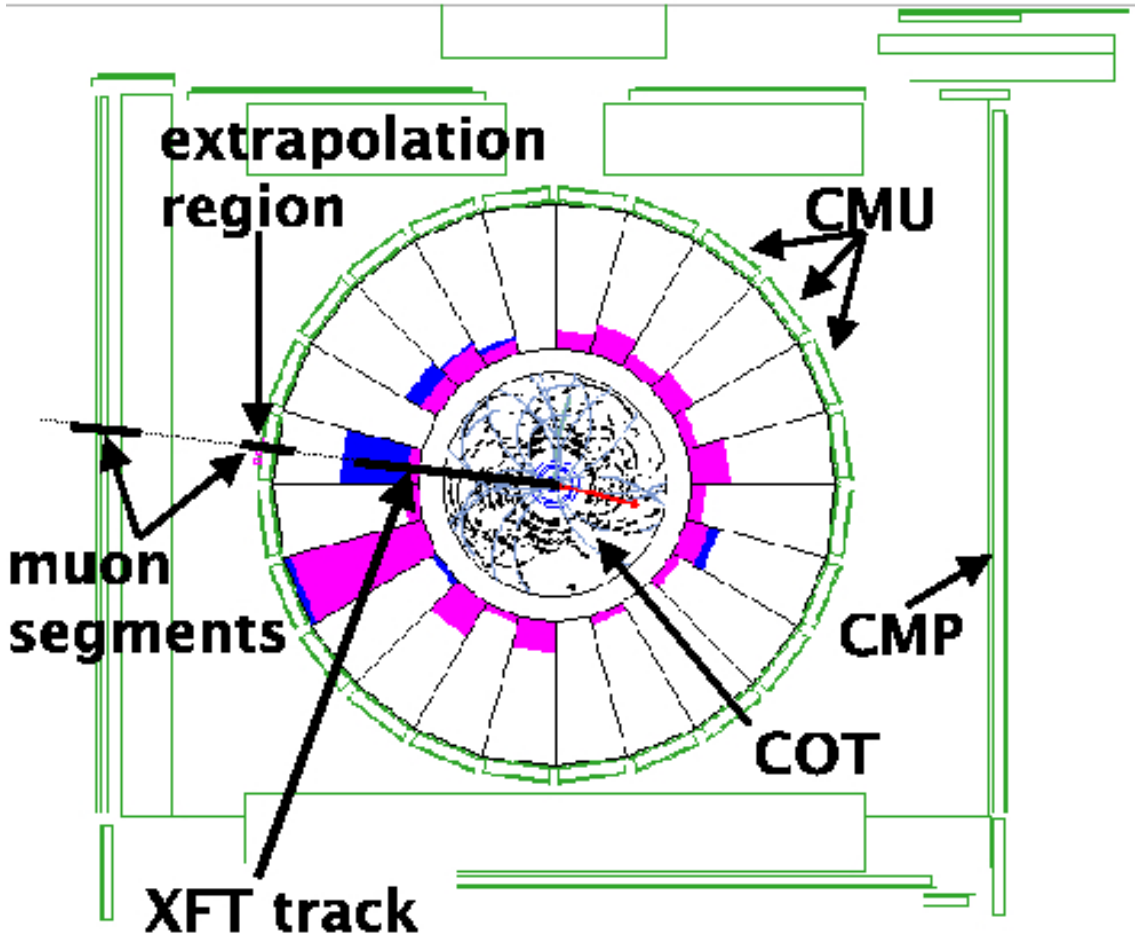


Fig. 9. A colliding beam event taken with the CDF-II detector. The event was accepted via a high- $p_T$  muon trigger path. The COT is shown at the center of the figure. There are several tracks observed with  $p_T < 1.5 \text{ GeV}/c$  that are reconstructed offline, but below the momentum threshold of the XFT. The one high momentum XFT track is identified pointing to the left in the figure. The central calorimeter energy is shown just outside the COT, followed by the CMU, shown as 24 rectangular detectors. The CMP is shown as the outer “box” shaped detector. The XFT track was extrapolated to the muon system and matched with track segments in the CMU and CMP detectors. The extrapolation “window” is shown as three small squares just outside the CMU detector. This indicates that the XTRP required a CMU stub within a  $6.3^\circ$  extrapolation window that accounts for curvature, misalignment and multiple scattering.

from the XFT, XTRP, SVT and Level-2 trigger systems. Checking that these track lists are identical to one another is a powerful tool to monitor the digital links between these systems. The 1Hz sampling of events is sufficient to identify problems without utilizing significant bandwidth. In the control room, XTRPMon provides monitoring histograms to the shift crew.

### 5.3 Performance

The XTRP system is performing as specified. Track matching to muons with a  $2.5^\circ$  granularity in the trigger allows for high purity single and dimuon triggers. Figure 9 shows a high momentum muon identified at the trigger level. Track matching to electrons with  $15^\circ$  granularity (followed by tighter matching at Level 2) allows for single and dielectron triggers. The Track-Trigger allows for single and two-track triggers based upon charged tracking information.

Overall, approximately 75% of the CDF-II trigger bandwidth utilized track-based triggers (electrons, muons and tracks) by way of the XTRP system. The flexibility of the look-up based extrapolation and trigger maps have allowed for improved and optimized trigger algorithms and matching parameters. The flexibility of the system firmware has also permitted algorithmic improvements.

### 5.4 Physics Impact

It is difficult to quantify the precise physics impact of different components of an integrated trigger system, but there are some aspects of the CDF-II physics program that require the full performance of the XTRP system:

- low-momentum dimuon triggers. We allow for muons with  $p_T > 1.5 \text{ GeV}/c$  for dimuon events, providing a large yield of  $J/\psi \rightarrow \mu^+\mu^-$  decays. This mode is important for  $B$  physics as well as detector calibration [15].
- high-momentum single muon triggers [16]. We allow for single muons with  $p_T > 4 \text{ GeV}/c$ . The trigger rate is manageable thanks to the precise matching that XTRP provides between the found tracks (XFT) and muon segments (L1 MUON). For muons with  $p_T = 10 \text{ GeV}/c$ , the extrapolation window in the trigger is approximately  $1^\circ$ , a precision that has never been achieved at the trigger level.
- single and di-electrons. With four possible electron thresholds, our standard thresholds are  $p_T = 8 \text{ GeV}/c$  for inclusive high momentum electrons,  $p_T = 4 \text{ GeV}/c$  for dilepton search triggers and semileptonic  $B$  decays, and  $p_T = 2 \text{ GeV}/c$  for  $J/\psi \rightarrow e^+e^-$  [17].
- track-only triggers. The CDF-II experiment has revolutionized hadron collider heavy flavor physics (charm, bottom) with the tracking trigger path that utilizes the Level 1 Track Trigger followed by the Level 2 Silicon Vertex Tracker. This has allowed large samples of hadronic charm and bottom decays to be identified. Hadronic heavy flavor physics was simply not accessible before this system was implemented [7].

The modularity of the CDF-II trigger system lends itself nicely to upgrades. We are currently commissioning the Track Trigger-II system, which will be a replacement to the Track Trigger system described in this document.

The design of the Track Trigger-II takes advantage of our experience with the XTRP/Track Trigger system and will be a direct replacement to the existing Track Trigger system. Improvements in SRAM technology, as well as faster, less expensive FPGA technology permit a design of the Track Trigger-II that will be able to process more tracks per event than the existing system. This is important at higher instantaneous Tevatron luminosity, because the track multiplicity grows with the number of interactions per bunch crossing. In addition, by performing data compression along with additional preprocessing, the Track Trigger-II is able to select events based upon the transverse mass of track-pairs. The new system provides a significant improvement in trigger performance, providing greater background rejection and better signal purity.

## **6 Conclusion**

We have developed a track extrapolation system and distribution system for the CDF-II trigger. The system was designed with testing, commissioning and monitoring in mind. The XTRP system has been functioning as part of the CDF-II trigger since the beginning of Tevatron Run II, and we anticipate it will remain an integral part of the trigger for the remainder of the run. The XTRP system, and the CDF-II trigger as a whole, are providing unprecedented data samples and access to physics channels never before observed.

We thank our colleagues on the CDF-II experiment, as well as the Fermilab staff. This work supported by Department of Energy, Contract DE-FG02-91ER40677.

## References

- [1] F. Abe et al., Phys.Rev.Lett. **74** 2626 (1995); S. Abachi et al., Phys.Rev.Lett. **74** 2632 (1995).
- [2] [http://www-fmi.fnal.gov/fmiinternal/MI\\_Technical\\_Design/index.html](http://www-fmi.fnal.gov/fmiinternal/MI_Technical_Design/index.html); G.Jackson, FERMILAB\\_TM-1991.
- [3] R. Blair et al., “The CDF-II Detector Technical Design Report,” FERMILAB-PUB-96-390-E (1996).
- [4] T. Affolder et al., Nucl. Inst. Meth. **A**526:249 (2004).
- [5] A. Bardi et al., Nucl. Inst. Meth. **A**285:178 (2002); W. Ashmanskas et al., Nucl. Inst. Meth. **A**518:532 (2004).
- [6] P. Azzi et al., Nucl. Inst. Meth. **A**419:532 (1998); A. Sill et al., Nucl. Inst. Meth. **A**447:1 (2000).
- [7] D. Acosta et al., Phys.Rev.Lett. **91**, 241804 (2003); D. Acosta et al., Phys. Rev. Lett. **95**:031801 (2005); A. Abulencia et al., hep-ex/0606027 (2006).
- [8] E.J. Thomson et al., “Online Track Processor for the CDF Upgrade,” IEEE Transactions on Nuclear Science, Vol. 49, No. 3 (2002).
- [9] ANSI/VIPA 23-1998, March 22, 1998.
- [10] Motorola MVME2301, MVME2401 and MVME5500 processors have been used, <http://www.motorola.com>.
- [11] National Semiconductor DS90CR281 28-bit Channel Link transmitter, <http://www.national.com>.
- [12] VxWorks is a product of WindRiver, <http://www.windriver.com>.
- [13] Jim Pangburn, “FISION v2.12 User’s Guide,” <http://www-cdfonline.fnal.gov/vme/FISION.html>;
- [14] RPC and Object Broker Interface (ROBIN), <http://www-cdfonline.fnal.gov/ROBINXXX.html>.
- [15] D. Acosta et al., Phys. Rev. Lett. **94**:101803 (2005); D. Acosta et al., Phys. Rev. Lett. **93**:072001 (2004).
- [16] D. Acosta et al., Phys. Rev. Lett. **94**:091803 (2005); D. Acosta et al., Phys. Rev. **D71**:051103 (2005).
- [17] D. Acosta et al., Phys. Rev. **D71**:052002 (2005); D. Acosta et al., Phys. Rev. **D71**:0702005 (2005).